Volume 4, Issue 1, pp. 1-5, 2020.

International Journal of Scientific Engineering and Science
ISSN (Online): 2456-7361

Thermo-Hydrodynamic (THD) Analysis of Oil Film Lubrication in the Connecting-Rod Big End Bearing

Trung Thien Pham[1*], Thị Thanh Hai Tran[2], Trong Thuan Luu[2]
[1]University of Economic and Technical Industries, Vietnam
[2]Hanoi University of Science and Technology, Vietnam
*Corresponding author email: ptthien.ck@uneti.edu.vn

***Abstract*— *This paper presents the theory and temperature calculation of the connecting-rod big end bearing in the experimental device. Using the numberical method, Reynolds equation solution model for the hydrodynamic bearing, and Reynolds boundary conditions for the erosion phenomenon and oil film flow interruption, the research can calculate the pressure of the bearing. On that basis along with using the energy equation, we can build the temperature calculation model of the oil film. The research carries out the temperature differences of the connecting-rod big end bearing oil film at different speeds. Also, it showes that the oil film temperature corresponds with the load on the connecting-rod. At the positon 0^o of the connecting-rod, the oil film temperature reaches the maximum value at the angle 360^o of the crankshaft, which is where the explosion happens. At the opposite position, which is the 180^o angle of the connecting-rod, the oil film temperature reaches the smallest value when the explosion happens because the oil film thickness is the biggest and the pressure is the smallest. At different positions of the connecting-rod, the temperature range decreases from the position $0^o$of the bearing to the position 180^o and increases gradually from the position $180^o$of the bearing to the position 360^o. The temperature increases a lot during the first working cycles, and after that when the bearing operates stably, the oil film temperature will increase slightly along with the working time of the bearing.*

***Keywords*— *Reynolds equation, energy equation, thermal effect, connecting-rod big end bearing.*

I. Introduction

Research to improve the efficiency and the lifetime of engine is a problem that has been concerned very much. To improve the lifetime of the engine, the lubrication for the connecting-rod big end bearing is the core problem. There are many factors affecting the lubrication of the connecting-rod big end bearing such as pressure, temperature ... Studying the temperature of lubricating oil film for the connecting-rod big end bearing helps us evaluate the efficiency of the engine by both numerical and empirical method.

In 1984, Booker and Shu [1] came up with a new approach for the calculation of elastic hydrodynamic lubrication. The approaches are based on a finite element method and they are applied directly to all shapes of the oil film with any complex load acting on the surface. In the same year, Goenka [2] presented a finite element method of calculating the lubrication mode, which reduces calculation time significantly. In 1985, Booker and Labouff [3] published a study about the inelastic and elastic bearing under dynamic load. In 1985, Fantino and Ash [4] made many comparisons between the activities of the two connecting-rod big end bearing with gasoline engine and diesel engine. In 1991, Fantino and his partners did a lot of calculation with the assumption that the bearing and the crankshaft didn't deformed, lubricating oil has a constant viscosity. The bearing operated transiently and under load dynamic gravity.

In 1986, Goenka and Oh [6] also mentioned the problem of hydrodynamic elastic lubrication. The method of authors was based on Rohde and Li's model [7]. The Newton- Raphson method and two numerical methods (finite and differential finite elements) were used to calculate approximately the Reynolds equation. In 1990, Kumar and his partners [8] studied, compared, and analyzed different methods about hydrodynamic elastic lubrication. In 1988, Mcivor and Fenner [9] researched and showed that the use of quadrilateral element 8 nodes save a lot off time compared to 3-button triangle. In 1992, Fenner and his teammates used the 8-node grid quadrilateral to analyze the oil film area and study the heavy bearing. The elastic deformation increases the range and thickness of oil film greatly and leads to a significant reduction of maximum pressure in the contact. In 2001, Bonneau and Hajjam [11] proposed an algorithm based on the model of JFO (Jakobson-Floberg and Olsson) and loosed discrete equations using finite element methods. This algorithm allows us to determine the disruption and regeneration of the oil film. The authors gave a modified Reynolds equation which can be applied to both the continuous and discontinuous regions of the oil film.

In this paper, the authors studied the temperature field of the lubricating oil film in the connecting-rod big end bearing which was calculated by numerical methods.

II. Theory Basis

A. *The Reynolds equation*

Reynolds's equation for a bearing under dynamic loads [8]:

$$\frac{\partial}{\partial x}\left(\frac{h^3}{12\mu}\frac{\partial p}{\partial x}\right)+\frac{\partial}{\partial y}\left(\frac{h^3}{12\mu}\frac{\partial p}{\partial y}\right)=U\frac{\partial h}{\partial x}+\frac{\partial h}{\partial t} \qquad (1)$$

Equation (1) is solved with boundary conditions. Reynolds took into account the disruption of the oil film (Figure 1).In the development domain include work zone (oil film zone continuously) and oil film area interrupted

Continuous region Ω has p> pcav (pcav is constant) is the area that axial surface and silver surfaces are completely separated by lubricating oil film.

The discontinuous zone Ω_0 which has p= pcav is an area mixed with air holes. In this region, the axial surface and

International Journal of Scientific Engineering and Science
Volume 1, Issue 1, pp. xx-xx, 2020. ISSN (Online): 2456-7361

silver are separated by a mixture of lubricating oil - gas.

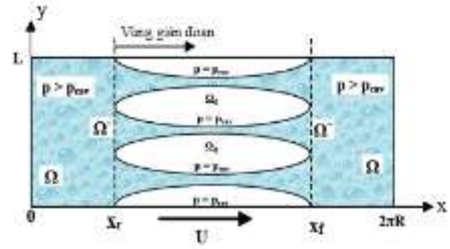

Fig. 1. The bearing deployment domain

At the discontinuity, the equation (1) is rewritten below:

$$U\frac{\partial \rho h}{\partial x}+2\frac{\partial \rho h}{\partial t}=0 \quad (2)$$

Where ρ is the specific gravity of the lubricating oil-gas

Let $r=\frac{\partial \rho h}{\rho_0}$ the thickness of the lubricating oil film gas, where ρ_0 is the specific gravity of the lubricant - gas mixture. The equation (2) becomes:

$$U\frac{\partial r}{\partial x}+2\frac{\partial r}{\partial t}=0 \quad (3)$$

The area between Ω và Ω_0 is the boundary Ω^+ and Ω^- and it begins the disruption and membrane restoration. Therefore, to determine the pressure distribution and find the discontinuity of the oil film, we have to solve the system of two equations (1) and (3) with two unknowns number p and r. Bonneau and Hajjam [8] gave unknown D which represented for both variables in continuous and discontinuous domains:

- For continuous oil film area

$$\begin{cases} D=p, D\geq 0 \\ F=1 \end{cases} \quad (4)$$

- For interrupted areas

$$\begin{cases} D=r-h, D<0\ (\rho<\rho_0) \\ F=0 \end{cases} \quad (5)$$

Thus, equations (1) and (3) are written as:

$$F\frac{\partial}{\partial x}\left(\frac{h^3}{12\mu}\frac{\partial D}{\partial x}\right)+F\frac{\partial}{\partial z}\left(\frac{h^3}{12\mu}\frac{\partial D}{\partial z}\right)=U\frac{\partial h}{\partial x}+\frac{\partial h}{\partial t}+(1-F)\left(\frac{U}{2}\frac{\partial D}{\partial x}+\frac{\partial D}{\partial t}\right) \quad (6)$$

B. The equation for the thickness of oil film

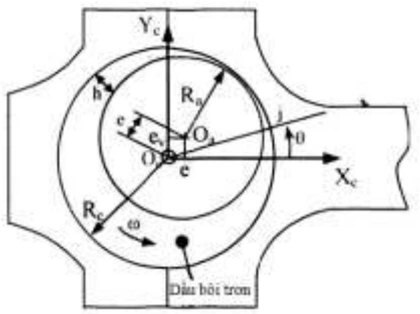

Fig. 2. The connecting-rod big end bearing cross section

The thickness of oil film h in Figure 2 is determined as follows:

$$h=C-e_{xe}cos\theta-e_{ye}sin\theta \quad (7)$$

In this equation, C= R_c-R_a (radical gap), e_x, và e_y is the coordinate of the center O_a. θ=x/R is the angular position of an M. Converting equation (7) to form:

$$h=C\left(1-\varepsilon_{xe}cos\theta-\varepsilon_{ye}sin\theta\right) \quad (8)$$

Where $\varepsilon_{xe}=e_{xe}/C$, $\varepsilon_{ye}=e_{ye}/$ is the relative eccentricity according to the coordinate axis of the center axis.

C. Load balancing equation.

Ignoring the inertial force, the equation balances the force acting on the transmission

$$\overrightarrow{F_{ext}}+\vec{F}_p=\vec{F}_{ext}+\int_S p\vec{n}\,dS=\vec{0} \quad (9)$$

Where F_{ext} is the external force, F_p is the generating hydrodynamic force.

Projecting equation (9) on two axes Xe, Ye we have the system load balancer:

$$\begin{cases} \int_S pcos\theta dS-F_{xe}=0 \\ \int_S psin\theta dS-F_{ye}=0 \end{cases} \quad (10)$$

D. Heat equation

Ignore heat transfer in perimeter and axial directions [6] [9], the energy equation has the form:

$$\delta C_p\left(u\frac{\partial T}{\partial x}+v\frac{\partial T}{\partial y}+w\frac{\partial T}{\partial z}\right)=\frac{\partial}{\partial y}\left(k\frac{\partial T}{\partial y}\right)+\mu\left[\left(\frac{\partial u}{\partial y}\right)^2+\left(\frac{\partial w}{\partial y}\right)^2\right] \quad (11)$$

Converting to dimensionless coordinates, we have :

$$\bar{u}\frac{\partial \bar{T}}{\partial \varphi}+\frac{1}{h}\left(\bar{v}-\bar{u}\bar{y}\frac{\partial \bar{h}}{\partial \varphi}\right)\frac{\partial \bar{T}}{\partial \bar{y}}+\bar{w}\frac{\partial \bar{T}}{\partial \bar{z}}=f_1\frac{1}{\bar{h}^2}\frac{\partial}{\partial \bar{y}}\left(\frac{\partial \bar{T}}{\partial \bar{y}}\right)+f_2\frac{\mu}{\bar{h}^2}\left[\left(\frac{\partial \bar{u}}{\partial \bar{y}}\right)^2+\left(\frac{\partial \bar{w}}{\partial \bar{y}}\right)^2\right] \quad (12)$$

Where:

$$Pe=\frac{\delta.\varphi.\omega.C^2}{k};\ f_1=\frac{k}{\delta.\varphi.\omega.C^2}=\frac{1}{Pe};\ N_e=\frac{R^2.\omega^2}{C_p.T_{in}};\ R_e=\frac{\delta.\varphi.\omega}{\mu_{in}};\ f_2=\frac{N_e}{R_e}$$

Velocity in directions of flow:

$$\bar{u}=\frac{\partial \bar{p}}{\partial \varphi}\left(\int_0^{\bar{y}}\frac{\bar{y}.\bar{h}^2}{\bar{\mu}}.d\bar{y}-\frac{\bar{F}_1}{\bar{F}_0}\int_0^{\bar{y}}\frac{\bar{h}^2}{\bar{\mu}}.d\bar{y}\right)+\bar{u}_1+\frac{\bar{u}_2-\bar{u}_1}{\bar{F}_0}\int_0^{\bar{y}}\frac{d\bar{y}}{\bar{\mu}}$$

$$\bar{w}=\frac{\partial \bar{p}}{\partial \bar{z}}\left(\int_0^{\bar{y}}\frac{\bar{y}.\bar{h}^2}{\bar{\mu}}.d\bar{y}-\frac{\bar{F}_1}{\bar{F}_0}\int_0^{\bar{y}}\frac{\bar{h}^2}{\bar{\mu}}.d\bar{y}\right)+\bar{w}_1+\frac{\bar{w}_2-\bar{w}_1}{\bar{F}_0}\int_0^{\bar{y}}\frac{d\bar{y}}{\bar{\mu}}$$

$$\bar{v}=-\int_0^{\bar{y}}\bar{h}.\left(\frac{\partial \bar{u}}{\partial \varphi}+\frac{\partial \bar{w}}{\partial \bar{z}}\right).d\bar{y}+v_1 \quad (13)$$

Where :

$$F=1-\int_0^1\frac{\bar{y}d\bar{y}}{\bar{\mu}}\Big/\int_0^1\frac{d\bar{y}}{\bar{\mu}}=1-F_3$$

$$F_2=\int_0^1\frac{\bar{y}}{\bar{\mu}}(\bar{y}-F_3)d\bar{y}$$

$$F_3=\frac{\int_0^1\frac{\bar{y}}{\bar{\mu}}d\bar{y}}{\int_0^1\frac{1}{\bar{\mu}}d\bar{y}}=\frac{\overline{F_1}}{\overline{F_0}}$$

The equation for conducting heat through silver has the form:

$$\frac{\partial^2 T_b}{\partial r^2}+\frac{1}{r}\cdot\frac{\partial T_b}{\partial r}+\frac{1}{r^2}\cdot\frac{\partial^2 T_b}{\partial \theta^2}+\frac{\partial^2 T_b}{\partial z^2}=0 \quad (14)$$

In dimensionless coordinates, the equation is written as following:

$$\frac{\partial^2 \bar{T}_b}{\partial \bar{r}^2} + \frac{1}{\bar{r}} \cdot \frac{\partial \bar{T}_b}{\partial \bar{r}} + \frac{1}{\bar{r}^2} \cdot \frac{\partial^2 \bar{T}_b}{\partial \bar{\theta}^2} + \frac{\partial^2 \bar{T}_b}{\partial \bar{z}^2} = 0 \quad (15)$$

Dimensionless variables are determined by the following expression:

$$\varphi = \frac{x}{R};\ \bar{z} = \frac{z}{R};\ \bar{y} = \frac{y}{h};\ \bar{h} = \frac{h}{C};\ \bar{u} = \frac{u}{\omega.R};\ \bar{v} = \frac{v}{\omega.C};\ \bar{w} = \frac{w}{\omega.K}$$

$$\bar{\mu} = \frac{\mu}{\mu_{in}};\ \bar{T} = \frac{T}{T_{in}};\ \bar{P} = \frac{P.C^2}{\mu_{in}.\omega.R^2};\ \bar{\beta} = \frac{\beta.C^2}{\mu_{in}.\omega.R^2}$$

According to Pierre [10], the thermal properties of the fluid are determined by the expression

$$\psi(\varphi, z) = (1 - g(\varphi, z)\psi(\varphi, z)_{air} + g(\varphi, z)\psi(\varphi, z)_{oil} \quad (16)$$

$\boldsymbol{\psi(\varphi, z)}$ includes the thermal properties of fluids such as thermal conductivity, specific heat, specific gravity, dynamic viscosity.

E. Boundary conditions.

The boundary conditions of the problem include the temperature condition at the shaft surface, silver surface and in the lubricating oil supply groove (Fig. 1). The conditions are written as following

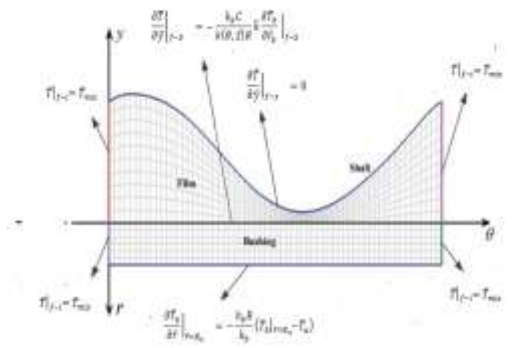

Fig. 3. Boundary condition

- On the surface between lubricant and silver:

$$\left.\frac{\partial \bar{T}}{\partial \bar{y}}\right|_{f-b} = -\frac{k_b C}{k(\theta, \bar{z})R} \bar{h} \left.\frac{\partial \bar{T}_b}{\partial \bar{r}_b}\right|_{f-b} \quad (17)$$

- On the contiguous surface between the lubricant film and the axis:

$$\left.\frac{\partial \bar{T}}{\partial \bar{y}}\right|_{f-s} = 0 \quad (18)$$

- At the lubricant supply channel:

$$\bar{T}|_{f-i} = \bar{T}_{mix} \quad (19)$$

$\bar{T}_{mix}$ is the oil temperature at the position of oil supply groove determined by the following formula:

$$T_{mix} = \frac{Q_{in}T_{in} + Q_{out}T_{out}}{Q_{in} + Q_{out}}$$

Where: Q_{in}, Q_{out} – oil flow in, outlet oil; T_{in}, T_{out} - temperature of input and output of the bearing

– On the outside of the silver:

$$\left.\frac{\partial \bar{T}_b}{\partial \bar{r}}\right|_{\bar{r}=R_n} = -\frac{h_b R}{k_b}\left(\bar{T}_b|_{\bar{r}=R_n} - \bar{T}_\alpha\right) \quad (20)$$

- On both sides of the silver:

$$\left.\frac{\partial \bar{T}_b}{\partial \bar{z}}\right|_{\bar{z}=0 \text{ or } 1} = -\frac{h_b R}{k_b}\left(\bar{T}_b|_{\bar{z}=0 \text{ or } 1} - \bar{T}_\alpha\right) \quad (21)$$

III. Modelization

A. Oil film temperature field

Development domain of the oil film changes from the real coordinate system to the dimensionless coordinates, natural coordinate system as the Figure 2 and Figure 3. The temperature at a point within the developed domain is interpolated according to the formula:

$$T^e = \sum_{i=1}^{s} N_i(r, \theta, z)T_i = \lfloor N \rfloor \{T\} \quad (22)$$

The interpolated functions Ni are written in a natural coordinate system

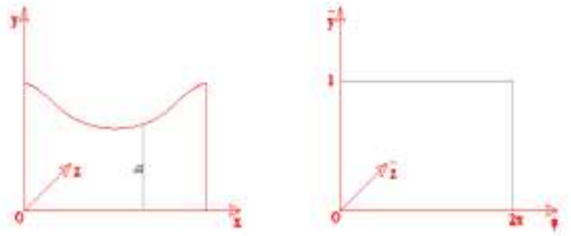

a.Real coordinate system *b. Dimentionless coordinate System*

Fig. 4. Oil film coordinate system

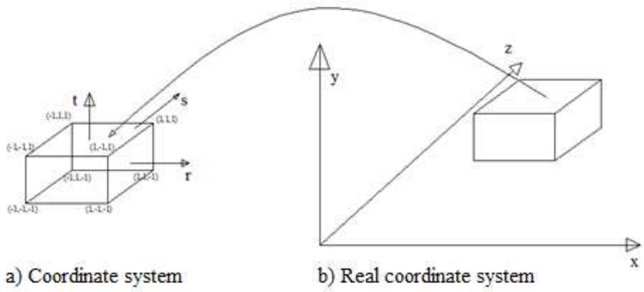

Fig. 5.Coordinate system convertsion

When changing from the real coordinate system to the natural coordinate system, we use the changing coordinate matrix Jacobi J. Therefore, the velocity of the oil film is determined as following:

$$\left\langle \begin{matrix} \bar{u} \\ \bar{w} \end{matrix} \right\rangle = J^{-1}.\left\langle \begin{matrix} \frac{\partial N_i}{\partial r} \\ \frac{\partial N_i}{\partial \delta} \end{matrix} \right\rangle.\{p_i\}.A_1 + \left\langle \begin{matrix} B_1 \\ B_2 \end{matrix} \right\rangle \quad (23)$$

$$\bar{v} = -\int_0^{\bar{y}} \bar{h}.\left\langle \frac{\partial N_i}{\partial \varphi}, \frac{\partial N_i}{\partial \bar{z}} \right\rangle.\left\{ \begin{matrix} \bar{u}_i \\ \bar{w}_i \end{matrix} \right\}.d\bar{y} + \bar{w}_1 \quad (24)$$

Where :

$$\begin{cases} \int_0^{\bar{y}} \frac{\bar{y}.\bar{h}^2}{\bar{\mu}}.d\bar{y} - \frac{\bar{F}_1}{\bar{F}_0}\int_0^{\bar{y}} \frac{\bar{h}^2}{\bar{\mu}}.d\bar{y} = A_1 \\ \bar{u}_1 + \frac{\bar{u}_2 - \bar{u}_1}{\bar{F}_0}\int_0^{\bar{y}} \frac{d\bar{y}}{\bar{\mu}} = B_1 \\ \bar{w}_1 + \frac{\bar{w}_2 - \bar{w}_1}{\bar{F}_0}\int_0^{\bar{y}} \frac{d\bar{y}}{\bar{\mu}} = B_2 \end{cases}$$

Galerkin finite element model for energy equation:

$$\iiint_v N_i\left(\bar{u}\frac{\partial \bar{T}}{\partial \varphi} + \frac{1}{\bar{h}}\left(\bar{v} - \bar{u}\bar{y}\frac{\partial \bar{h}}{\partial \varphi}\right)\frac{\partial \bar{T}}{\partial \bar{y}} + \bar{w}\frac{\partial \bar{T}}{\partial \bar{z}} - \right.$$

International Journal of Scientific Engineering and Science
Volume 1, Issue 1, pp. xx-xx, 2020. ISSN (Online): 2456-7361

$$\frac{f_1}{\bar h^2}\frac{\partial}{\partial y}\left(\frac{\partial \bar T}{\partial \bar y}\right) - f_2\frac{\bar\mu}{\bar h^2}\left[\left(\frac{\partial\bar u}{\partial\bar y}\right)^2+\left(\frac{\partial\bar w}{\partial\bar y}\right)^2\right] d\varphi d\bar y d\bar z = 0 \quad (25)$$

Converting equation (25), we have:

$$K = \iiint_{v_i} N_i.\left(\bar u.\frac{\partial N_i}{\partial\varphi} + \frac{1}{\bar h}\left(\bar v - \bar u\bar y\frac{\partial\bar h}{\partial\varphi}\right)\frac{\partial N_i}{\partial\bar y} + \bar w\frac{\partial N}{\partial\bar z}\right).dv_i\{T_i\} \quad (26)$$

$$K_1 = \iiint_{v_i}\frac{f_1}{\bar h^2}.\left\langle\frac{\partial N_i}{\partial\bar y}\right\rangle.\left\{\frac{\partial N_i}{\partial\bar y}\right\}.dv.\{T_i\} + \iint_{bạc}\frac{f_1}{\bar h^2}.N_i.\frac{\partial N}{\partial\bar y}.ds.\{T_i\} \quad (27)$$

$$f = \iiint_{v_i} N_i.f_2.\frac{\bar\mu}{\bar h^2}\left[\left(\frac{\partial\bar u}{\partial\bar y}\right)^2+\left(\frac{\partial\bar w}{\partial\bar y}\right)^2\right].dv \quad (28)$$

Finally, we obtain the system of equations:

$$(K + K_1)\{T_i\} = f \quad (29)$$

Solving the system of equations (29), we get the temperature field of oil film

B. The temperature field of the bearing

Applying the Galerkin finite element model to the equation of the heat transfer of silver as following:

$$\iiint\{N_i\}\left(\frac{\partial^2 T_b}{\partial r^2} + \frac{1}{r}\cdot\frac{\partial T_b}{\partial r} + \frac{1}{r^2}\cdot\frac{\partial^2 T_b}{\partial\theta^2} + \frac{\partial^2 T_b}{\partial z^2}\right) r.dr.d\theta.dz = 0 \quad (30)$$

Developing equation (26) we have:

$$\iiint_V \{N_i\}\frac{\partial^2 T_b}{\partial r^2} r.dr.d\theta.dz = \iint_S \{N\}\frac{\partial T}{\partial r} r.d\theta.dz\Big|_{R_t}^{R_n} - \iiint_V \left\{\frac{\partial N}{\partial r}\right\}\left\langle\frac{\partial N}{\partial r}\right\rangle r.dr.d\theta.dz\{T_i\} \quad (31)$$

$$\iiint_V \{N_i\}\frac{\partial^2 T_b}{\partial z^2} r.dr.d\theta.dz = \iint_S \{N\}\frac{\partial T}{\partial z} r.dr.d\theta\Big|_{z=0}^{z=1} - \iiint_V \left\{\frac{\partial N}{\partial z}\right\}\left\langle\frac{\partial N}{\partial z}\right\rangle r.dr.d\theta.dz\{T_i\} \quad (32)$$

$$\iiint_V \{N_i\}\frac{1}{r^2}\frac{\partial^2 T}{\partial\theta^2} r.dr.d\theta.dz = \iint_S \{N\}\frac{1}{r}\frac{\partial T}{\partial\theta} r.dr.dz\Big|_0^{2\pi} - \iiint_V \left\{\frac{\partial N}{\partial\theta}\right\}\frac{1}{r}\left\langle\frac{\partial N}{\partial\theta}\right\rangle r.dr.d\theta.dz\{T_i\} \quad (33)$$

$$\iiint_V \{N_i\}\frac{1}{r}\frac{\partial T}{\partial r} r.dr.d\theta.dz = \iiint_V \{N_i\}\left\langle\frac{\partial N}{\partial r}\right\rangle.dr.d\theta.dz\{T_i\} \quad (34)$$

Combining (27), (28), (29), (30), we get the system of equations:

$$K_b.\{T\}_b = f_b \quad (35)$$

Solving this system of equations (35), we get the heat field degree of silver.

IV. RESULTS

The configuration of the connecting-rod big end bearing:

Configuration	Value	Unit
Diameter inside the bearing (d)	97	mm
Diameter outside the bearing (D)	118	mm
Length of the bearing (L)	20	mm
Radical gap diameter (C)	0,038	mm
Eccentricity similarity (ε)	0,3-0,6-0,9	
Intermittent zone pressure ($\boldsymbol{p_c}$)	0	Pa
Modulus constant(β)	10^8	Pa
Kinematic viscosity (μ)	0,135	Pa.s
Thermal conductivity coefficient of oil	0,13	W/m.^{0}K
Density of oil	970	Kg/m^3
Specific heat capacity of oil	2000	J/Kg.^{0}K
Viscosity reduction coefficient with temperature	0,034	1/^{0}C
Silver thermal conductivity	100	W/m.^{0}K
Convection coefficient of silver	80	W/m^2.^{0}K
Rotation speed (n)	100-200	rpm
Environmental temperature	26	^{0}C
Supply oil temperature	26	^{0}C

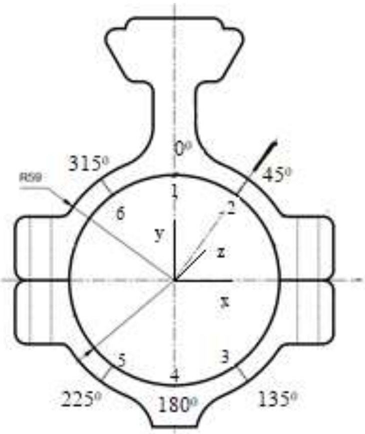

Fig. 6. Position of Connecting-rod angle

Fig. 7: Oil film field temperature at 100 rpm. The bearing temperature reaches its maximum value at 0° angle of the connecting rod. Oil film temperature reaches minimum at 180^0 of the connecting rod. With rotation speed at 100rpm, the largest temperature difference in the bearing is 3^0 C.

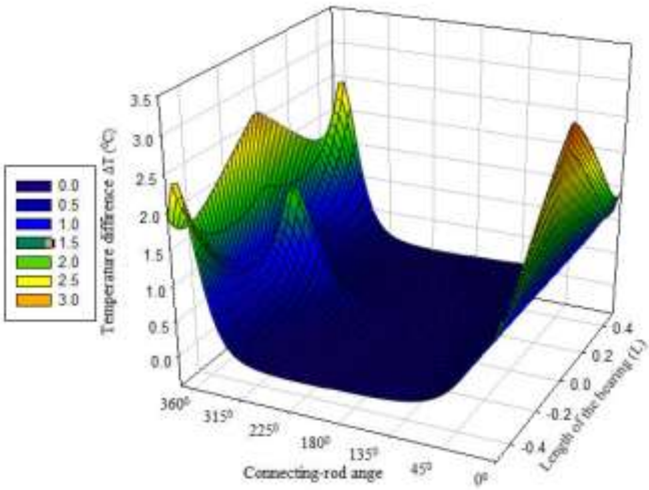

Fig. 7. Temperature field of oil film at 100 rpm

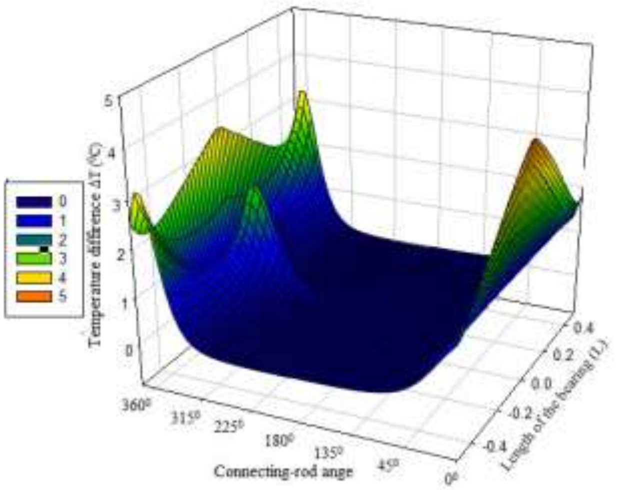

Fig. 8. Temperature field of oil film at 150 rpm

Fig. 8: Oil film temperature at 150 rpm. With 150 rpm

rotation speed the largest temperature difference in the bearing is 4.2^0 C.

The color table next to the temperature diffirence column shows the maximum increase in temperature with yellow

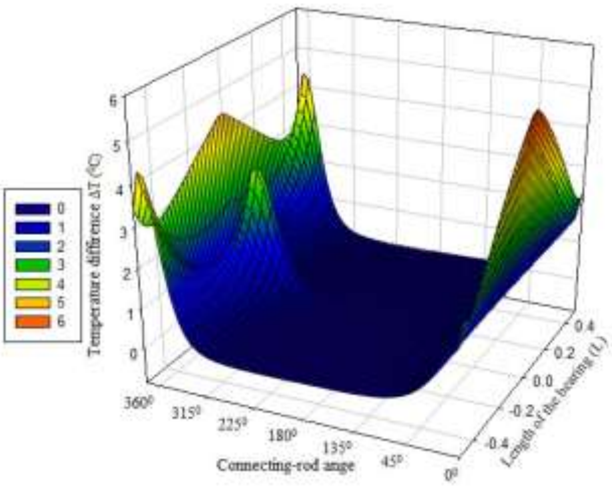

Fig. 9. Temperature field of oil film at the speed 200 rpm

Fig. 9: The temperature field of the oil film at 200 rpm has the largest temperature difference in the bearing (5.1^{0C}). When the spindle is clockwise, the temperature area at 0^0 and 360^0 of of the connecting-rod big end bearing the maximum value. The temperature zone at 135^0 and 180^0 of the connecting rod has the minimum value The temperature zone at 225^0 and 315^0 of connecting-rod is bigger than this at 135^0 and 180^0 of connecting rod.

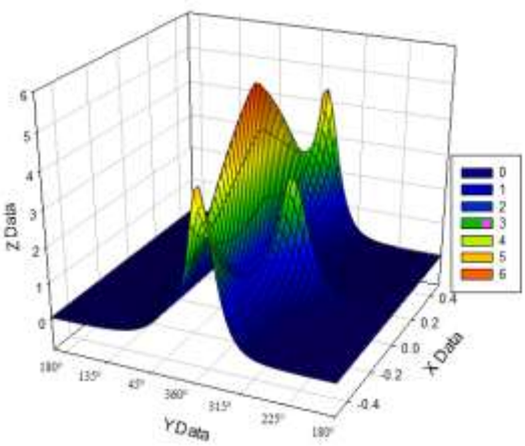

Fig. 10. Temperature field of oil film at the speed 200 rpm

Figure 10 (X Data: length of bearing, Y Data: The connecting-rod angle, Z Data: Temperature difirence) perimeter with the angle of view diffirent. The same figure 9, when the spindle is clockwise, the temperature area at 360^0 of the connecting-rod big end bearing the maximum value. The temperature zone at 180^0 of of the connecting-rod big end bearing has the minimum.

Caculation shows the results of the temperature field of the oil film in the connecting-rod big end bearing. According to the circumference of the bearing (Connecting-rod angle), the temperature reaches its maximum value at the center of the bearing (the 0^0 angle of the connecting-rod). It is the place where the explosion occurs; the oil film temperature is the highest. The temperature of the oil film gradually decreases on both sides. At 180^0 of the connecting-rod, the oil film temperature is lowest. The higher the rotation speed is, the greater the temperature increases. At the angular position of 0^0 of the connecting-rod when the thickness of oil film is lowest, the pressure value is highest and the oil film temperature is largest, too. The calculation results are completely consistent with hydrodynamic lubrication theory.

REFERENCES

[1] BOOKER J. F., SHU C. F., Finite element analysis of transient elastohydrodynamic lubrication, Proc. 10-th Leeds-Lyon Symposium on Tribology Developments in numerical and experimental method applied to Tribology, p. 157-163, 1984.

[2] GOENKA, P.K., *Dynamically Loaded Journal Bearings: Finite Element Method Analysis*, Transaction of the ASME, Journal of Lubrication Technology, vol. 106, p. 429-439, 1984.

[3] LABOUFF G. A., BOOKER J. F., *Dynamically loaded journal bearings: a finite element treatment for rigid and elastic surfaces*, Transaction of the ASME, Journal of Tribology, vol. 107, No.4, p. 505-515, 1985.

[4] FANTINO B., FRENE J., *Comparison of Dynamic Behaviour of Elastic Connecting-rod Bearing in Both Petrol and Diesel Engines*, Transaction of the ASME, Journal of Tribology , Vol.107, p. 87-91, 1985.

[5] FANTINO B., DU PARQUET J., FRENE J., Comportement dynamique d'un palier de tête de bielle élastiquement déformable: comparaison de deux méthodes de calcul, Revue Science et Industrie, Paris, FRANCE (1970-1993), No. 438, p. 22-24, 1991.

[6] GOENKA, P.K., OH K.P., An optimum short bearing theory for the *elastohydrodynamic solution of journal bearings*, Transaction of the ASME, Journal of Tribology, Vol 108, p. 294-299, 1986.

[7] ROHDE S. M., LI D. F., *A Generalized Short Bearing Theory*, Transaction of the ASME, Journal of Tribology , vol. 102, No.3, p. 278-280, 1980.

[8] KUMAR A., GOENKA, P.K., BOOKER J.F., *Modal Analysis of lastohydrodynamic Lubrication: A Connecting Rod Application*, Transaction of the ASME, Journal of Tribology, Vol. 112, p. 3524–534, 1990.

[9] MCIVOR J.D.C., FENNER D.N., An evolution of eight-node quadrilateral finite elements for the analysis of a dynamically loaded hydrodynamic journal bearing, Proc. Inst. Mech. Engrs., vol. 202, p. 95-101, 1988.

[10] FENNER D. N., MCIVOR J. D. C., CONWAY-JONES J. M., XU H., *The effect of compliance on peak oil film pressure in connecting rod bearings*, Proc. 19th Leeds-Lyon Symposium on Tribology, Leeds, September 1992.

[11] BONNEAU D., HAJJAM M., Modélisation de la rupture et de la réformation des films lubrifiants dans les contacts élastohydrodynamiques, Revue Européenne des Eléments Finis, Vol. 10, p. 679-704, 2001

[12] Dowson, D., A Generalized Reynolds Equation for Fluid-Film Lubrication. Int. J. Mech. Sci., Pergamon Press Ltd., Vol. 4, pp. 159-170, 1967